Engineering Turbulencw Modelling and Expriments 6

pp. 319–328, Eds. W. Rodi, M. Mulas, Elsevier, 2005

HYBRID LES-RANS: COMPUTATION OF THE FLOW AROUND A THREE-DIMENSIONAL HILL

L. Davidson [a] and S. Dahlström [a]

[a]Department of Thermo and Fluid Dynamics
Chalmers University of Technology, SE-412 96 Göteborg, Sweden
http://www.tfd.chalmers.se/~lada

ABSTRACT

The main bottle neck for using Large Eddy Simulations at high Reynolds number is the requirement of very fine meshes near walls. Hybrid LES-RANS was invented to get rid of this limitation. In this method unsteady RANS (URANS) is used near walls and at a certain distance from the wall, where the LES resolution is sufficiently good, a switch to LES is made. A one-equation RANS turbulence model is used in the URANS region and a one-equation SGS model is employed in the LES region. The matching between URANS and LES takes place in the inner log-region.

In the present paper an improved LES-RANS method is evaluated for computing the flow over a three-dimensional axi-symmetric hill. The improvement consists of adding instantaneous turbulent fluctuations (forcing conditions) at the matching plane between the LES and URANS regions in order to provide the equations in the LES region with relevant turbulent structures. The turbulent fluctuations are taken from a channel DNS. Three different approaches are compared in the present paper: hybrid LES-RANS with forcing conditions, hybrid LES-RANS without forcing conditions, and LES employing the WALE SGS model

KEYWORDS

LES, hybrid LES-RANS, DES, forcing conditions, 3D hill, URANS

INTRODUCTION

When simulating bluff body flows, LES (Large Eddy Simulations) is the ideal method. Bluff body flows are dominated by large turbulent scales which can be resolved by LES without too fine resolution and accurate results can be obtained at affordable cost (Rodi et al., 1997; Krajnović and Davidson, 2003, 2004). On the other hand, doing accurate predictions of wall-bounded flows with LES is a challenging task. The near-wall grid spacing should be about one wall unit in the wall-normal direction. This is similar to the requirement in RANS (Reynolds-Averaged Navier-Stokes) using low-Re number models. The resolution requirement in wall-parallel planes for a well-resolved LES in the near-wall region expressed in wall units is approximately 100 (streamwise) and

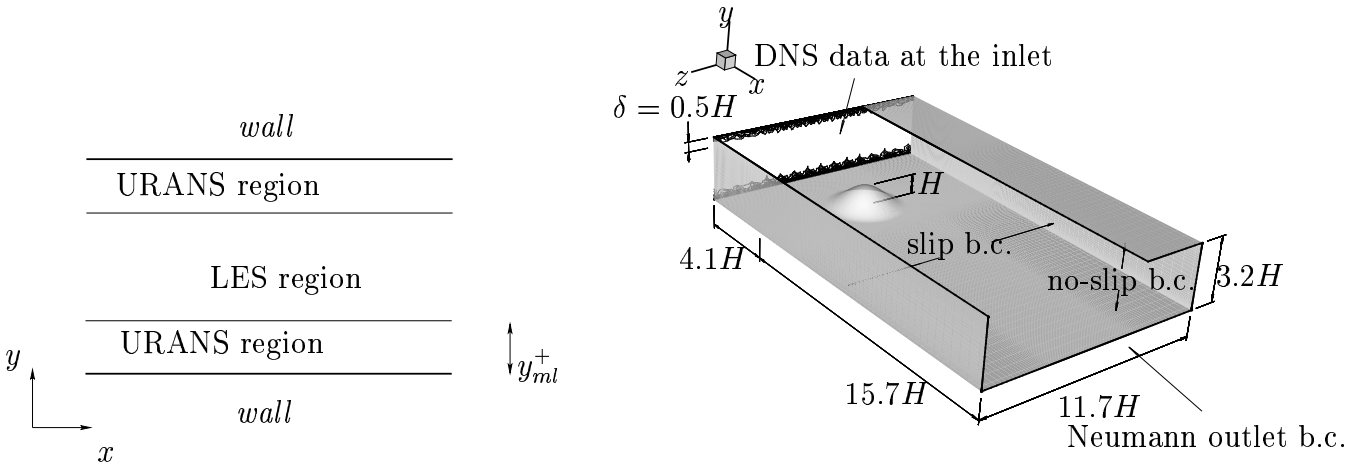

Figure 1: The LES and URANS region (left) and the computational domain (right).

20 (spanwise). This enables resolution of the near-wall turbulent structures in the viscous sublayer and the buffer layer consisting of high-speed in-rushes and low-speed ejections (often called the streak process). At low to medium Reynolds numbers the streak process is responsible for the major part of the turbulence production. These structures must be resolved in an LES in order to get accurate results. Thus, for wall-bounded flows at high Reynolds numbers of engineering interest, the computational resource requirement of accurate LES is prohibitively large. Indeed, the requirement of near-wall grid resolution is the main reason why LES is too expensive for engineering flows, which was one of the lessons learnt in the LESFOIL project (Davidson et al., 2003; Mellen et al., 2003).

The object of hybrid LES-RANS (Xiao et al., 2003; Davidson and Peng, 2003; Temmermann et al., 2002; Tucker and Davidson, 2004; Tucker, 2003) is to get rid of the requirement of high near-wall resolution in wall-parallel planes. In the near-wall region (the URANS region), a low-Re number RANS turbulence model (usually an eddy-viscosity model) is used. In the outer region (the LES region), the usual LES is used, see Fig. 1. The idea is that the effect of the near-wall turbulent structures should be predicted by the RANS turbulence model rather than being resolved. The matching between the URANS region and the LES region usually takes place in the inner part of the logarithmic region. In the LES region, coarser grid spacing in wall-parallel planes can be used. In this region the grid resolution is presumably dictated by the requirement of resolving the largest turbulent scales in the flow (which are related to the outer length scales, e.g. the boundary layer thickness), rather than the near-wall turbulent processes. The unsteady momentum equations are solved throughout the computational domain. The turbulent RANS viscosity is used in the URANS region, and the turbulent SGS viscosity is used in the LES region.

Although good results have been presented with hybrid LES-RANS, it has been found that the treatment of the interface between the URANS region and the LES region is crucial for the success of the method. The resolved turbulence supplied by the URANS region to the LES region does not have any reasonable turbulent characteristics and is not representative of turbulence at all. This results in too poorly resolved stresses on the LES side of the interface and this gives a hack – also referred to as a shift – in the velocity profile approximately at the location of the matching plane.

In Dahlström (2003); Davidson and Dahlström (2004) and Davidson and Billson (2004) an improved hybrid LES-RANS was presented in which fluctuations were added – taken either from channel DNS or synthesized – at the LES side of the interface. The method was applied to flow

in a channel and in an asymmetric diffuser. The method was shown to give good agreement with experimental results. An interesting – and rather similar approach – was recently presented by Batten et al. (2004) in which synthetic turbulent fluctuations was used to trig the resolved turbulence when going from an URANS region to an LES region.

In the present paper three different methods are evaluated for computing the flow over a three-dimensional axi-symmetric hill, see Fig. 1: hybrid LES-RANS with forcing conditions, hybrid LES-RANS without forcing conditions and LES using the WALE SGS model. The predictions are compared with experiments of Simpson et al. (2002) and Byun et al. (2003, 2004).

It can be mentioned that a wide range of turbulence models were applied to this flow including many different two-equation eddy-viscosity models, the explicit algebraic Reynolds stress model and a full Reynolds stress model. All RANS models fail completely in capturing this flow (Haase et al., 2005).

EQUATIONS

The Navier-Stokes equations with an added turbulent/SGS viscosity read

$$\frac{\partial \bar{u}_i}{\partial t} + \frac{\partial}{\partial x_j}\left(\bar{u}_i \bar{u}_j\right) = \delta_{1i} - \frac{1}{\rho}\frac{\partial \bar{p}}{\partial x_i} + \frac{\partial}{\partial x_j}\left[\left(\nu + \nu_T\right)\frac{\partial \bar{u}_i}{\partial x_j}\right], \quad \frac{\partial \bar{u}_i}{\partial x_i} = 0 \tag{1}$$

where $\nu_T = \nu_t$ (ν_t denotes the turbulent RANS viscosity) for $y \leq y_{ml}$ (see Fig. 1), otherwise $\nu_T = \nu_{sgs}$. The turbulent viscosity ν_T is computed from an algebraic turbulent length scale and for k_T a transport equation is solved, see below. The density is set to one in all simulations.

HYBRID LES–RANS

A one-equation model is employed in both the URANS region and LES region which reads

$$\frac{\partial k_T}{\partial t} + \frac{\partial}{\partial x_j}(\bar{u}_j k_T) = \frac{\partial}{\partial x_j}\left[\left(\nu + \nu_T\right)\frac{\partial k_T}{\partial x_j}\right] + P_{k_T} - C_\varepsilon \frac{k_T^{3/2}}{\ell}, \quad P_{k_T} = -\tau_{ij}\bar{s}_{ij}, \quad \tau_{ij} = -2\nu_T \bar{s}_{ij} \tag{2}$$

where $\nu_T = c k^{1/2} \ell$. In the inner region ($y \leq y_{ml}$) k_T corresponds to RANS turbulent kinetic energy k; in the outer region ($y > y_{ml}$) it corresponds to subgrid-scale kinetic turbulent energy (k_{sgs}). No special treatment is used in the equations at the matching plane except that the form of the turbulent viscosity and the turbulent length scale are different in the two regions. At walls $k_T = 0$. More details in Davidson and Dahlström (2004).

Forcing conditions

The DNS fluctuations are added as momentum sources in the cells in the LES region adjacent to the matching plane. The sources for the three momentum equations read

$$S_U = -\gamma \rho u'_{DNS} v'_{DNS} A_n, \quad S_V = -\gamma \rho v'_{DNS} v'_{DNS} A_n, \quad S_W = -\gamma \rho w'_{DNS} v'_{DNS} A_n \tag{3}$$

where A_n is the area of the control volume, and $\gamma = c_\gamma k_T(x, y_{ml}, z)/k_{fluct}$, where k_{fluct} is the turbulent kinetic energy of the DNS fluctuations and $c_\gamma = 0.4$. The time history of the channel DNS database along a line y_{ml} is used. The streamwise variation is obtained by employing Taylor's hypothesis. These DNS fluctuations are consider to be generic, i.e. to be used for all types of flow. The object of the DNS fluctuations is to act as a forcing term, and as such the exact form of the fluctuations is not critical: the forcing term should force the momentum equations to start

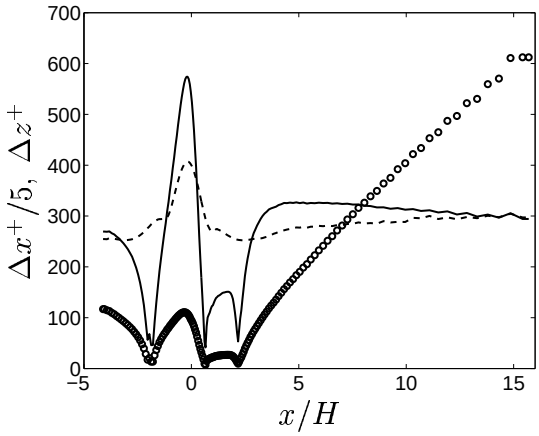

(a) —— Δz^+ at $z = 0$; - - - Δz^+ at $z/H = 1.65$; ∘: $\Delta x^+/5$ at $z = 0$.

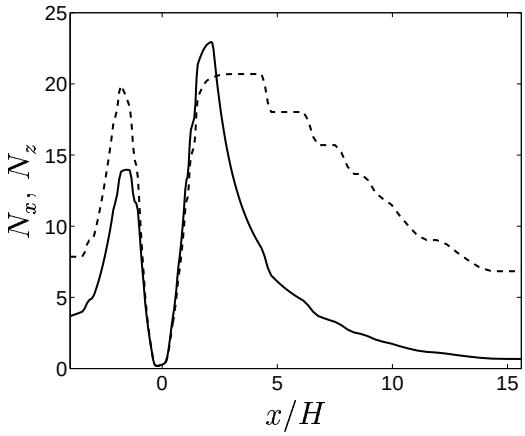

(b) —— $N_x = (\delta_{95}/\Delta x)_{z=0}$; - - - $N_z = (\delta_{95}/\Delta z)_{z=0}$.

Figure 2: Grid spacings.

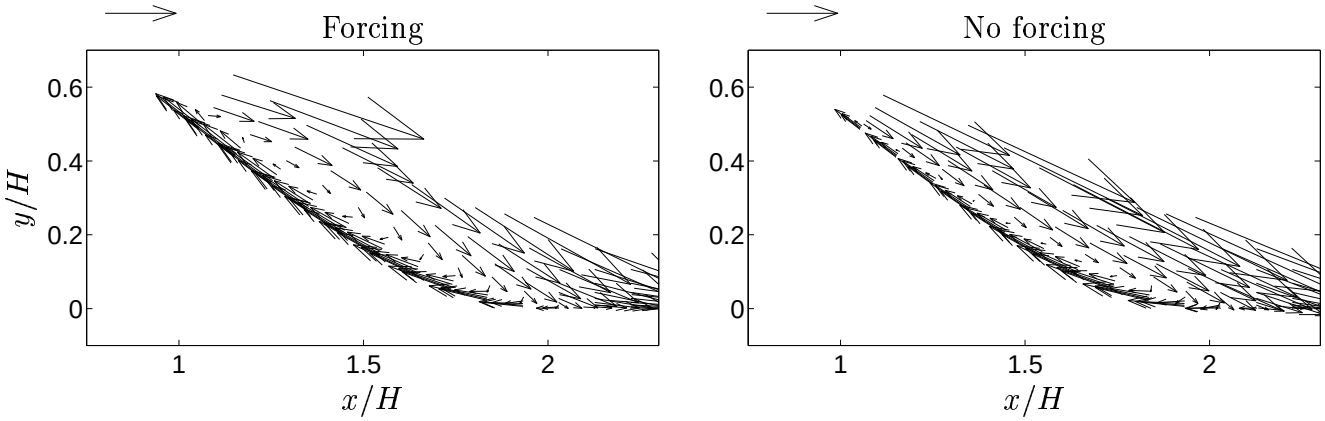

Figure 3: Velocity vectors in symmetry plane. Every 2^{nd} vector in x direction and every 3^{rd} vector in y direction are shown. The vectors above the figures have the magnitude of $0.1U_{in}$.

to resolve large-scale turbulence. The forcing term should be physical, i.e. in some sense mimic turbulent fluctuations, but it is probably also important that its time scale and length scale are related to the that of grid cells. There is no point in using a forcing term whose length scale is much larger or smaller than the computational cell, because such a term cannot trigger the equations into resolving turbulence.

The location of the interface is set to $y^+ \simeq 40$ at the inlet, and in the domain it is defined by the time averaged streamline starting at this y-location. More details can be found in Davidson and Dahlström (2004) and Davidson and Billson (2004).

The Numerical Method

An incompressible, finite volume code is used (Davidson and Peng, 2003). For space discretization, central differencing is used for all terms. The Crank-Nicolson scheme (with $\alpha = 0.6$) is used for time discretization of all equations. The numerical procedure is based on an implicit, fractional step technique with a multigrid pressure Poisson solver Emvin (1997) and a non-staggered grid arrangement.

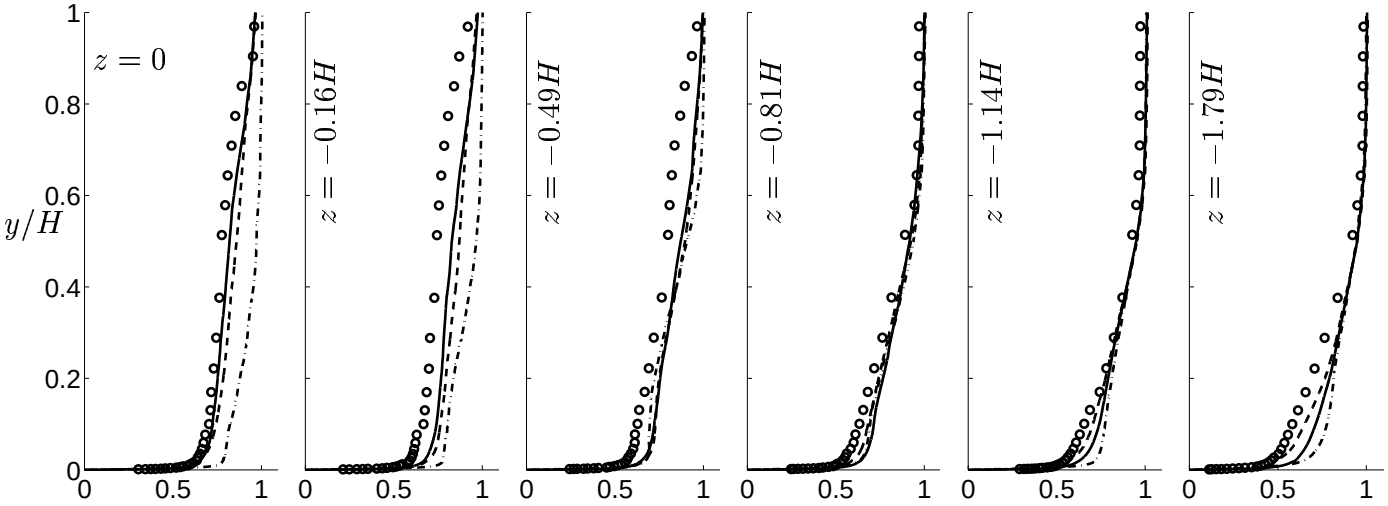

Figure 4: Streamwise velocity component $\langle \bar{u} \rangle / U_{in}$ at $x = 3.69H$. — hybrid LES-RANS with forcing; - - - hybrid LES-RANS without forcing; - - - LES; ∘ experiments (Simpson et al., 2002)

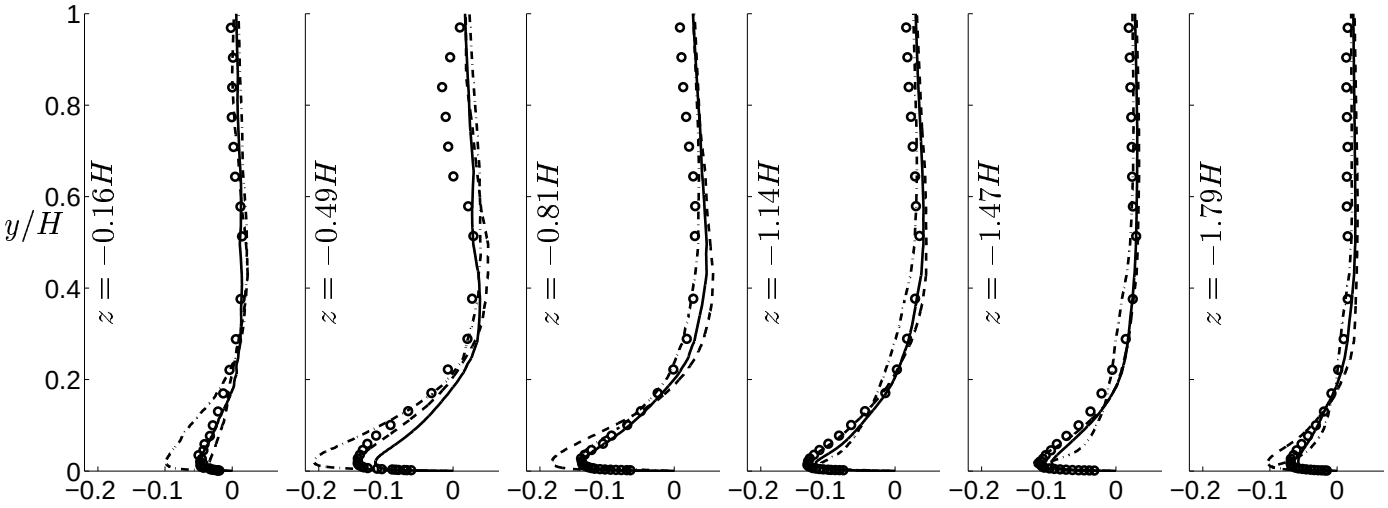

Figure 5: Spanwise velocity component $\langle \bar{w} \rangle / U_{in}$ at $x = 3.69H$. — hybrid LES-RANS with forcing; - - - hybrid LES-RANS without forcing; - - - LES; ∘ experiments (Simpson et al., 2002)

RESULTS

A $162 \times 82 \times 130$ (x, y, z) mesh is used (1.7 million cells). It is nearly orthogonal in the near-wall region of the hill. The inlet is located at $x = -4.1H$ and the outlet at $x = 15.7H$, see Fig. 1. The mean inlet $\langle \bar{u} \rangle$ profile is set according to experimental data (measured at $x = 0$ without hill). Instantaneous turbulent fluctuations are taken from a channel DNS of $Re_\tau = u_\tau \delta / \nu = 500$ (Davidson and Dahlström, 2004). The flow in the lower half of the channel flow (half width δ) is then used to superimpose turbulent fluctuations in the boundary layers at the lower and upper wall. It turned out that RMS of the instantaneous fluctuations from the channel DNS matched the experimental RMS profiles reasonably well and no re-scaling of was applied. Slip conditions are used at the side walls and homogeneous Neumann conditions are employed for all variables at the outlet.

A time step of $\Delta t U_{in}/H = 0.026$ is used which gives a maximum instantaneous CFL of approximately 2 (the CFL number is larger than 1 in approximately 100 cells). The computations are run 8 000 time steps to make sure that the flow is fully developed which corresponds to 10 through flows. The flow is then time averaged during 5000 time steps. An estimate if this is sufficient is

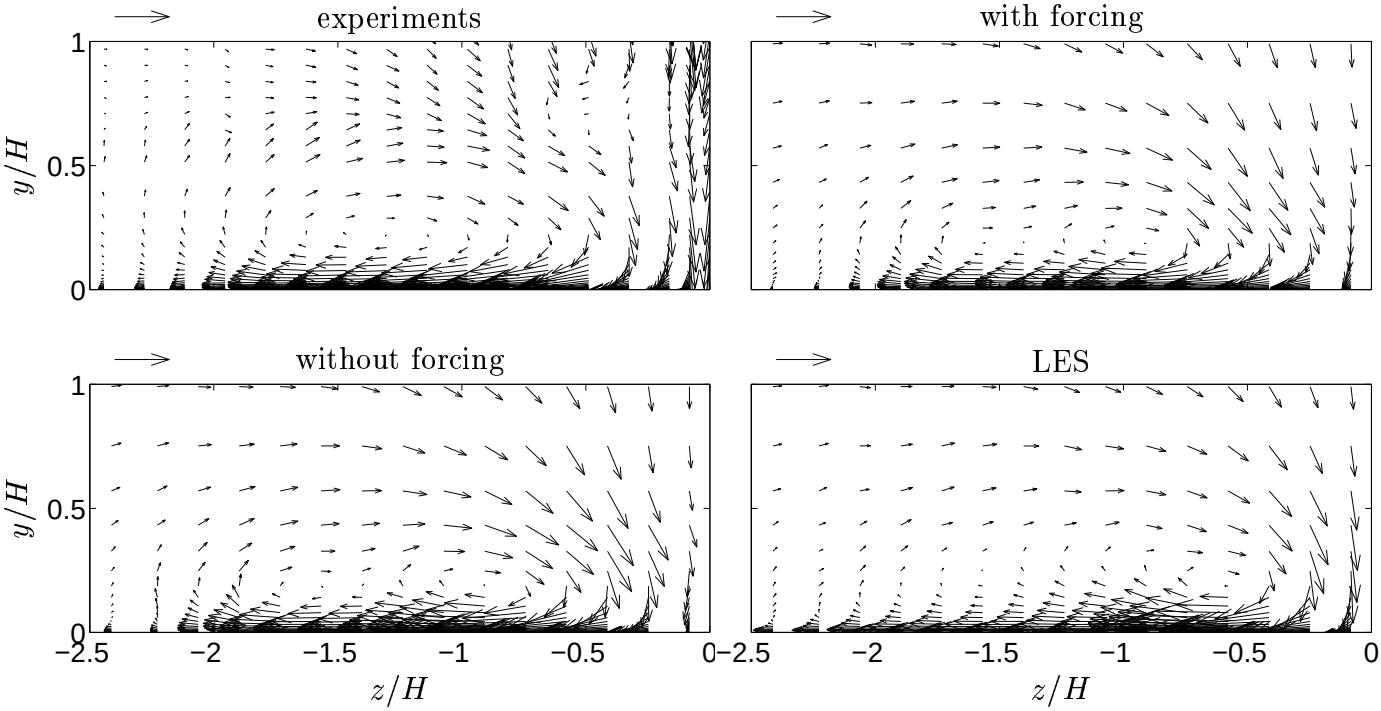

Figure 6: $\langle\bar{v}\rangle$–$\langle\bar{w}\rangle$ velocity vectors. $x/H = 3.69$. Every 3^{rd} and 2^{nd} vector in z and y direction, respectively, are shown. The vectors above the figures have the magnitude of $0.1U_{in}$.

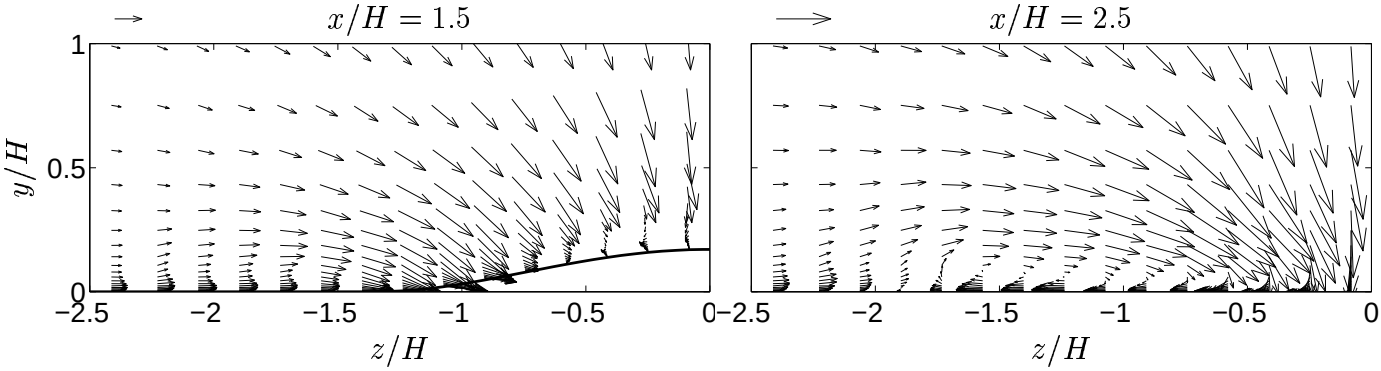

Figure 7: $\langle\bar{v}\rangle$–$\langle\bar{w}\rangle$ velocity vectors at $x/H = 1.5$ and $x/H = 2.5$. Hybrid LES-RANS with forcing. Every 3^{rd} and 2^{nd} vector in z and y direction, respectively, are shown. The vectors above the figures have the magnitude of $0.1U_{in}$.

to check how symmetric the flow is. A qualitative answer is obtained by looking at the spanwise velocity component at plane $x = 3.69H$, see Fig. 5. For example, after sampling during 5 000 time steps the maximum asymmetry in the $\langle\bar{w}\rangle$ profile is $0.027U_{in}$ and occurs near the symmetry plane at $|z|/H = 0.16$, where the flow is highly unsteady. Two global iterations are required for each time step and the CPU time for one time step is 25 seconds on a single AMD Opteron 244 processor.

Some details of the grid are shown in Fig. 2. The streamwise and spanwise grid spacing in wall units are, as can be seen, fairly large, with the latter varying between 200 and 300, except at the foot and the crest of the hill. The Δx^+ values start at around 500 at the inlet, and attains values of 40 in the recirculating region. When we look at the grid spacings expressed as the ratio of the boundary layer thickness and the grid spacing we find values between 5 and 20 in the hill region for

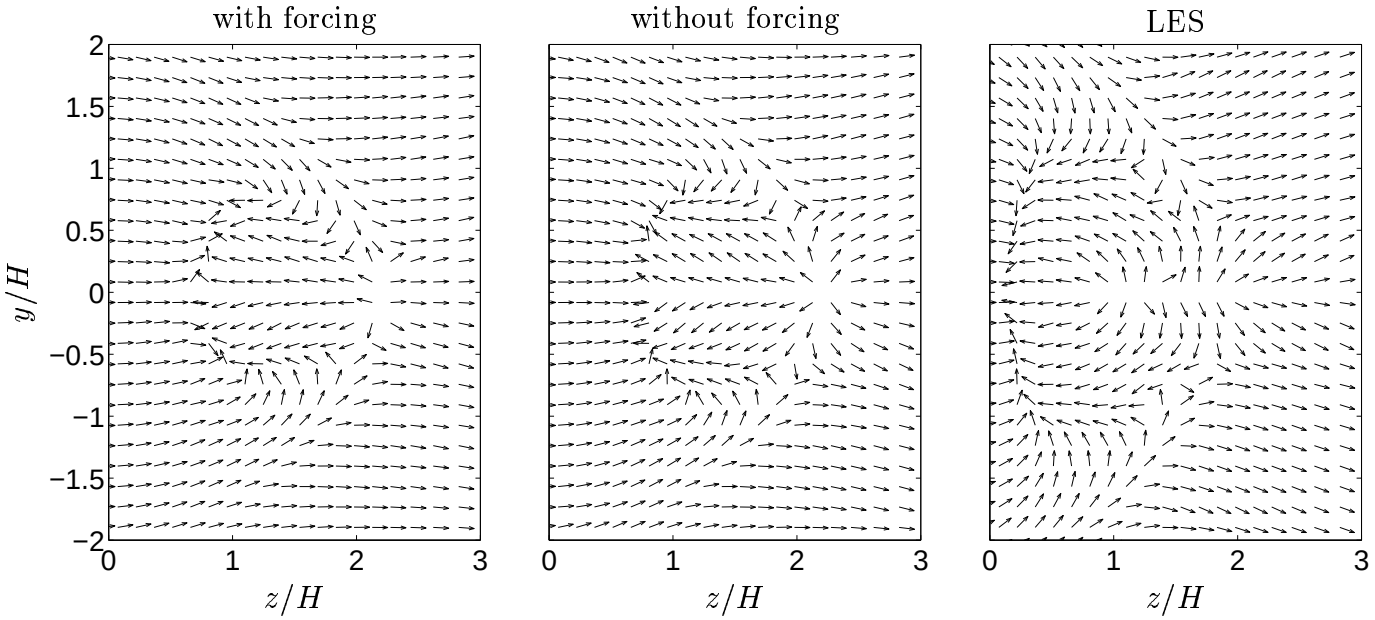

Figure 8: Unit velocity vectors ($\langle\bar{u}\rangle$ – $\langle\bar{w}\rangle$) along the lower wall. Every 3^{rd} vector in x and z direction are shown.

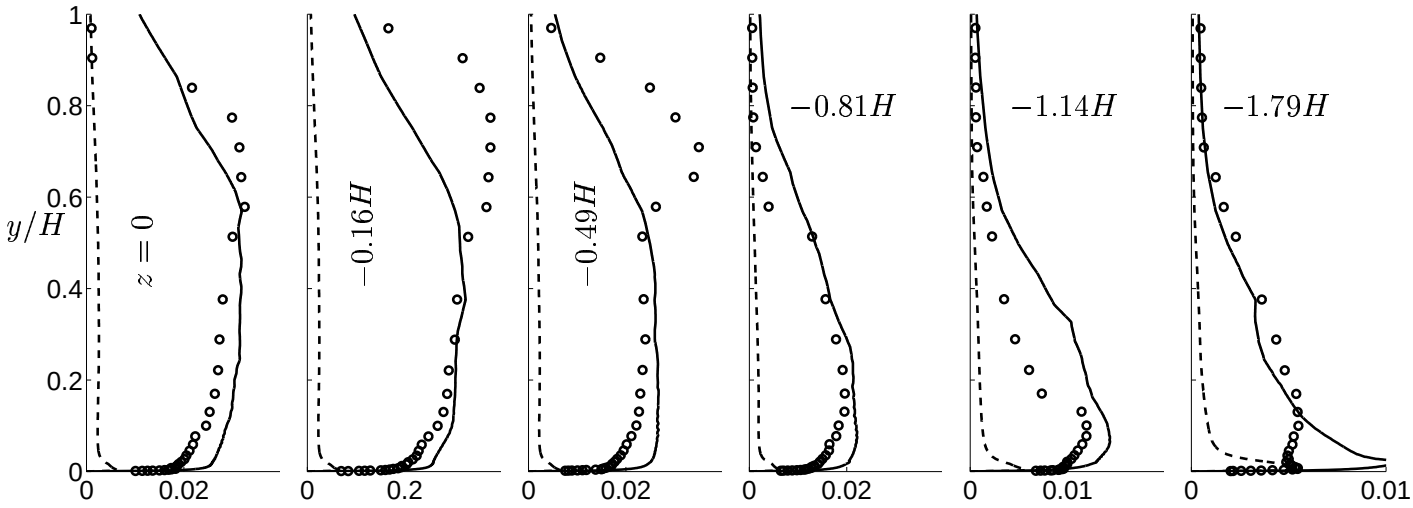

Figure 9: Turbulent kinetic energy. Hybrid LES-RANS with forcing. $x/H = 3.69$. —— resolved energy $0.5\langle u_i' u_i'\rangle / U_{in}^2$; - - - modelled energy k_T/U_{in}^2; ∘ experiments (Simpson et al., 2002).

both N_x and N_z, except at the separation region where δ_{95} goes to zero (Fig. 2b). The object with hybrid LES-RANS and DES is to free the grid spacing of the Reynolds number dependence, and make it dependent only of outer scalings. Spalart et al. (1997) suggest that the value of N_x and N_z for a well-resolved LES should be 20, assuming that the viscous-influenced region is accurately modelled with (U)RANS. $N_x \simeq N_z \simeq 8$ was used in the airfoil simulations by Dahlström (2003).

Vector fields in the symmetry plane $z = 0$ are shown for the hybrid LES-RANS with and without forcing conditions in Fig. 3. The separation region for the LES simulations takes place earlier and is much shorter (not shown). The flow separates at $x/H \simeq 1$ and re-attaches at $x/H \simeq 2$ both with and without forcing. This is in reasonable good agreement with LDV measurement of Byun et al. (2003).

Figure 4 presents the streamwise velocities at $x/H = 3.69$. Fairly good agreement is obtained with the hybrid LES-RANS, both with and without forcing. The LES simulations give a slightly worse

agreement with experiments. The predicted velocity profiles in all simulations are too full. This indicates either too a slow predicted recovery rate or too a small predicted recirculation bubble. It can also be seen that all predicted velocity profiles in Fig. 4 are larger than the experimental velocities. The reason for this difference is not clear.

The secondary velocity fields at $x = 3.69H$ are presented in Figs. 5 and 6. The overall agreement between predictions and experiments is rather good. The magnitude of the predicted $\langle \bar{w} \rangle$ by LES are too large at $z/H \geq -0.49$ compared with experiments. The velocity fields in Fig. 6 for both hybrid LES-RANS predictions and experiments show a large clock-wise vortex whose centre is located at $y/H \simeq 0.2$, $z/H \simeq -1.2$. The centre for the LES simulations, however, is located too close to the centre, compared with experiments. The main difference between the hybrid LES-RANS simulations and the experiments is found in the central region at $y/H \simeq 0.7$, $z/H \simeq -0.5$. Here the large clock-wise vortex in the experiments is broken, and it looks like a trace of a decaying counter clock-wise vortex (it is also clearly seen in the experimental spanwise velocity profile at $z/H = -0.49$ in Fig. 5). No such vortex is visible in the predictions.

In Fig. 7 the secondary velocity fields are presented for $x/H = 1.5$ and $x/H = 2.5$. Here it can be seen that at $x/H = 2.5$ a streamwise vortex has been created induced by the reattaching flow in the symmetry plane. It has its centre at $z/H \simeq -1.3$, and it gets larger further downstream (cf. Fig. 6). No vortex is present at $x/H = 1.5$. The streamwise vortex predicted with hybrid LES-RANS without forcing (not shown) is very similar to that in Fig. 7, whereas the streamwise vortex predicted with LES (also not shown) is virtually non-existent.

The direction of the flow at the wall is visualized in Fig. 8. Here the flow patterns observed in the symmetry plane and the cross planes are recognized. The flow approaches the hill and is forced to diverge in the lateral direction ($\pm z$ direction). For the two hybrid LES-RANS simulations a recirculating region is formed at $1 \lesssim x/H \lesssim 2$, $|z|/H \lesssim 0.5$ (slightly wider without forcing), whereas that predicted with LES is much larger.

Figure 9 shows the turbulent kinetic energies. As can be seen, the agreement between predictions and experiments is good. The largest discrepancies are seen in the central region for $-0.16 \geq z/H \geq -0.49$, $y/H \gtrsim 0.5$, in which the experimental values are considerable larger than the predicted ones. This is probably related to the trace of a experimental streamwise counter clock-wise vortex observed in Fig. 6 which was not seen in the predictions. This vortex could be responsible for generation of turbulent kinetic energy which is advected downstream. It could also be that the position of the vortex is unsteady, which would show up as high turbulent kinetic energy.

As can be seen from Fig. 9 the modelled turbulence is much smaller than the resolved one, except close to the wall at $z/H \leq -1.14$.

CONCLUSIONS

Two hybrid LES-RANS methods – one standard and one in which DNS fluctuations are added as forcing conditions – and one LES with the WALE model have been used to predict the flow around a three-dimensional axi-symmetric hill. A mesh of 1.7 million cells is used. The two hybrid methods give both results which are in fairly good agreement with experiments. The agreement of the LES results with experiments slightly worse but still acceptable. As mentioned in the Introduction, steady RANS simulations fail completely.

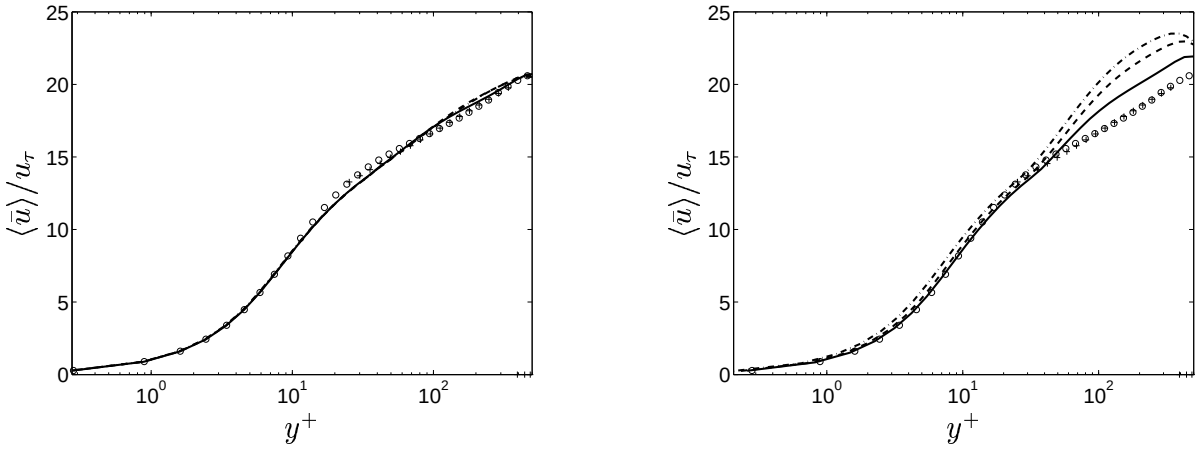

(a) Forcing. (b) No forcing.

Figure 10: Channel flow. $Re_\tau = u_\tau \delta / \nu = 500$. — $x/\delta = 7$; - - - $x/\delta = 15$; - · - $x/\delta = 23$; ∘ DNS (Davidson and Dahlström, 2004); +: $2.5 \ln(y^+) + 5.2$.

It has earlier been found that standard hybrid LES-RANS (i.e. without forcing) gives rather poor results for channel flow, whereas when forcing conditions are employed the agreement is excellent (Davidson and Dahlström, 2004; Davidson and Billson, 2004). It is thus somewhat surprising that for the 3D hill flow hybrid LES-RANS without forcing gives as good results as with forcing conditions. This was also found for the flow in the plane, asymmetric diffuser (Davidson and Dahlström, 2004).

Standard hybrid LES-RANS performs poorly in fully developed channel flow (periodic boundary conditions), because the only boundary that the LES region sees is the interface to the URANS region, and the turbulence that is transported across this boundary represents a poor turbulent boundary condition. On the contrary, both in the diffuser flow and the 3D hill flow realistic turbulence is imposed as inlet boundary conditions. Of course, if the inlet is situated very far upstream, the flow will forget the inlet boundary conditions, but in both the diffuser flow and the 3D hill flow, the inlet is located rather close to the expansion and the hill, respectively. In Fig. 10, the two hybrid LES-RANS methods are used to compute *developing* flow in a channel. Instead of using periodic boundary conditions in the streamwise direction, inlet and outlet conditions are used. Instantaneous inlet boundary conditions are prescribed from channel DNS data (Davidson and Dahlström, 2004). Velocity profiles are shown for three streamwise locations downstream of the inlet, namely $x/\delta = 7, 15$ and $x/\delta = 23$. As can be seen, the agreement for the hybrid LES-RANS with forcing conditions is perfect at all three locations thanks to the added DNS fluctuations at the interface, whereas in the hybrid LES-RANS simulations without forcing conditions the resolved turbulence is gradually dissipated. The distance from the inlet to the hill foot in the present 3D hill simulations is approximately 2δ. In the diffuser simulations the distance between the inlet to the start of the expansion (diffuser region) is 16δ.

Acknowledgments.
This work was financed by the FLOMANIA project (Flow Physics Modelling – An Integrated Approach) and is a collaboration between Alenia, AEA, Bombardier, Dassault, EADS-CASA, EADS-Military Aircraft, EDF, NUMECA, DLR, FOI, IMFT, ONERA, Chalmers University, Imperial College, TU Berlin, UMIST and St. Petersburg State University. The project is funded by the European Union and administrated by the CEC, Research Directorate-General, Growth Programme, under Contract No. G4RD-CT2001-00613.

REFERENCES

Batten, P., Goldberg, U., Chakravarthy, S., 2004. Interfacing statistical turbulence closures with large-eddy simulation. AIAA Journal 42 (3), 485–492.

Byun, G., Simpson, R., Long, C. H., 2003. A study of vortical separation from three-dimensional symmetric bumps. AIAA paper 2003-0641, Reno, N.V.

Byun, G., Simpson, R., Long, C. H., 2004. A study of vortical separation from three-dimensional symmetric bumps. AIAA Journal 42 (4), 754–765.

Dahlström, S., 2003. Large eddy simulation of the flow around a high-lift airfoil. Ph.D. thesis, Dept. of Thermo and Fluid Dynamics, Chalmers University of Technology, Göteborg, Sweden. [1]

Davidson, L., Billson, M., 2004. Hybrid LES/RANS using synthesized turbulence for forcing at the interface. In: Neittaanmäki, P., Rossi, T., Korotov, S., Oñate, E., Périaux, J., Knörzer, D. (Eds.), ECCOMAS 2004. July 24-28, Finland. [1]

Davidson, L., Cokljat, D., Fröhlich, J., Leschziner, M., Mellen, C., Rodi, W. (Eds.), 2003. LESFOIL: Large Eddy Simulation of Flow Around a High Lift Airfoil. Vol. 83 of Notes on Numerical Fluid Mechanics. Springer Verlag.

Davidson, L., Dahlström, S., 2004. Hybrid LES-RANS: An approach to make LES applicable at high Reynolds number (keynote lecture). In: de Vahl Davis, G., Leonardi, E. (Eds.), CHT-04: Advances in Computational Heat Transfer III. April 19-24, Norway. [1]

Davidson, L., Peng, S.-H., 2003. Hybrid LES-RANS: A one-equation SGS model combined with a $k-\omega$ model for predicting recirculating flows. International Journal for Numerical Methods in Fluids 43, 1003–1018.

Emvin, P., 1997. The full multigrid method applied to turbulent flow in ventilated enclosures using structured and unstructured grids. Ph.D. thesis, Dept. of Thermo and Fluid Dynamics, Chalmers University of Technology, Göteborg. [1]

Haase, W., Aupoix, B., Bunge, U., Schwamborn, D. (Eds.), 2005. FLOMANIA: Flow-Physics Modelling – An Integrated Approach. Notes on Numerical Fluid Mechanics and Multidisciplinary Design. Springer.

Krajnović, S., Davidson, L., 2003. Numerical study of the flow around the bus-shaped body. ASME: Journal of Fluids Engineering 125, 500–509.

Krajnović, S., Davidson, L., 2004. Large eddy simulation of the flow around an Ahmed body. In: 2004 ASME Heat Transfer/Fluids Engineering Summer Conference. Charlotte, USA. [1]

Mellen, C., Fröhlich, J., Rodi, W., 2003. Lessons from LESFOIL project on large eddy simulation of flow around an airfoil. AIAA Journal 41 (4), 573–581.

Rodi, W., Ferziger, J., Breuer, M., Pourquié, M., 1997. Status of large-eddy simulations: Results of a workshop. J. Fluids Engineering, 248–262.

Simpson, R., Long, C. H., Byun, G., 2002. Study of vortical separation from an axisymmetric hill. International Journal of Heat and Fluid Flow 23 (5), 582–591.

Spalart, P., Jou, W.-H., Strelets, M., Allmaras, S., 1997. Comments on the feasability of LES for wings and on a hybrid RANS/LES approach. In: Liu, C., Liu, Z. (Eds.), Advances in LES/DNS, First Int. conf. on DNS/LES. Greyden Press, Louisiana Tech University.

Temmermann, L., Leschziner, M., Hanjalić, K., 2002. A-priori studies of near-wall RANS model within a hybrid LES/RANS scheme. In: Rodi, W., Fueyo, N. (Eds.), Engineering Turbulence Modelling and Experiments 5. Elsevier, pp. 317–326.

Tucker, P., 2003. Differential equation based length scales to improve DES and RANS simulations. AIAA paper 2003-3968, 16th AIAA CFD Conference.

Tucker, P., Davidson, L., 2004. Zonal k-l based large eddy simulation. Computers & Fluids 33 (2), 267–287.

Xiao, X., Edwards, J., Hassan, H., 2003. Inflow boundary conditions for LES/RANS simulations with applications to shock wave boundary layer interactions. AIAA paper 2003–0079, Reno, NV.

[1] can be downloaded from www.tfd.chalmers.se/~lada